

---

## Field guide across the exhumed Himalayan mid-crust along the Tama Kosi and Rolwaling valleys of east-central Nepal

*Larson K. and Kellett D.*

Journal of the VIRTUAL EXPLORER, Electronic Edition, ISSN 1441-8142, volume 47, Paper 14, DOI: 10.3809/jvirtex.2014.00339, In: (Eds) Chiara Montomoli, Rodolfo Carosi, Rick Law, Sandeep Singh, and Santa Man Rai, Geological field trips in the Himalaya, Karakoram and Tibet, 2014.

---

Download from: <http://www.virtualexplorer.com.au/article/2014/339/tama-kosi-and-rolwaling-valleys-east-central-nepal/index.html>

Click <http://virtualexplorer.com.au/subscribe/> to subscribe to the Virtual Explorer  
Email [team@virtualexplorer.com.au](mailto:team@virtualexplorer.com.au) to contact a member of the Virtual Explorer team

---

Copyright is shared by The Virtual Explorer Pty Ltd with authors of individual contributions. Individual authors may use a single figure and/or a table and/or a brief paragraph or two of text in a subsequent work, provided this work is of a scientific nature, and intended for use in a learned journal, book or other peer reviewed publication. Copies of this article may be made in unlimited numbers for use in a classroom, to further education and science. The Virtual Explorer Pty Ltd is a scientific publisher and intends that appropriate professional standards be met in any of its publications.



## Field guide across the exhumed Himalayan mid-crust along the Tama Kosi and Rolwaling valleys of east-central Nepal

Larson K.<sup>1</sup> and Kellett D.<sup>2</sup>

<sup>1</sup> Earth and Environmental Sciences, University of British Columbia, Okanagan, 3333 University Way, Kelowna, BC, Canada, V1V 1V7.

<sup>2</sup> Geological Survey of Canada, 601 Booth Street, Ottawa, ON, Canada, K1A 0E8.

### GUIDE INFO

#### Keywords

Inverted metamorphic gradient  
Main Central Thrust  
Lesser Himalaya  
Greater Himalaya

#### Citation

Larson, K. and Kellett, D. 2014. Field guide across the exhumed Himalayan mid-crust along the Tama Kosi and Rolwaling valleys of east-central Nepal. In: (Eds.) Chiara Montomoli, Rodolfo Carosi, Rick Law, Sandeep Singh, and Santa Man Rai, Geological field trips in the Himalaya, Karakoram and Tibet, Journal of the Virtual Explorer, Electronic Edition, ISSN 1441-8142, volume 47, paper 14, DOI: 10.3809/jvirtex.2014.00339

#### Correspondence to:

kyle.larson@ubc.ca

### IN THIS GUIDE

The upper Tama Kosi and Rolwaling valleys in east-central Nepal expose the exhumed mid-crustal core of the Himalayan orogen. The region provides an easily accessible transect across, and good exposure of rocks preserved within that core. Traveling northward from Dolakha in the south to the Tibet border in the north, the rocks record an inverted metamorphic field gradient ranging from chlorite-grade phyllite at lowest structural levels to sillimanite-grade migmatite and leucogranite at the uppermost structural levels. Rocks along this transect are pervasively deformed and preserve dominantly south-directed thrust shear sense indicators. Moreover, they are interrupted by a metamorphic, deformational, and geochronologic discontinuity. Investigation of such structures has helped to reveal the processes responsible for assembly of the Himalayan mid-crust and evolution of the present day kinematic framework. Moreover, integration of available field, microstructural, petrochronologic, and pressure-temperature data has provided insight into the relationship between processes accommodating foreland - hinterland convergence. This field guide describes a number of exposures along the Tama Kosi and Rolwaling valleys in which the deformation, metamorphism, and anatexis at various different structural positions can be observed and compared.

### INTRODUCTION

The Himalaya represent an unparalleled natural laboratory for examining processes active in large continent-continent collisional zones. The massive topographic relief and rock exposure along orogen-perpendicular river valleys form vertical structural cross-sections through the mountain range. These transects expose a variety of lithotectonic units including foreland basins deposits, deformed supracrustal sedimentary rocks, the now exhumed high-grade mid-crustal infrastructure of the orogen, and overlying, detached and deformed sedimentary cover. With the exception of the lower crust, by following a transect across the Himalaya one has the opportunity to walk through and examine a wide range of rock types

involved in mountain building process at almost any structural level.

This virtual field guide traverses the upper Tama Kosi and Rolwaling valley region of east-central Nepal (Figure 1), a region underlain by the exhumed, mid-crustal metamorphic core of the orogen. The transect along the Tama Kosi and Rolwaling river valleys crosses the well-documented Himalayan inverted metamorphic sequence which contains and a structure in the metamorphic package that is expressed as a structural, chronologic, and metamorphic discontinuity (Larson et al., 2013). Potentially similar discontinuities have recently been reported from various structural positions across the Himalaya (e.g. far east Nepal - Goscombe et al., 2006; central Nepal - Larson et al., 2010; west central Nepal

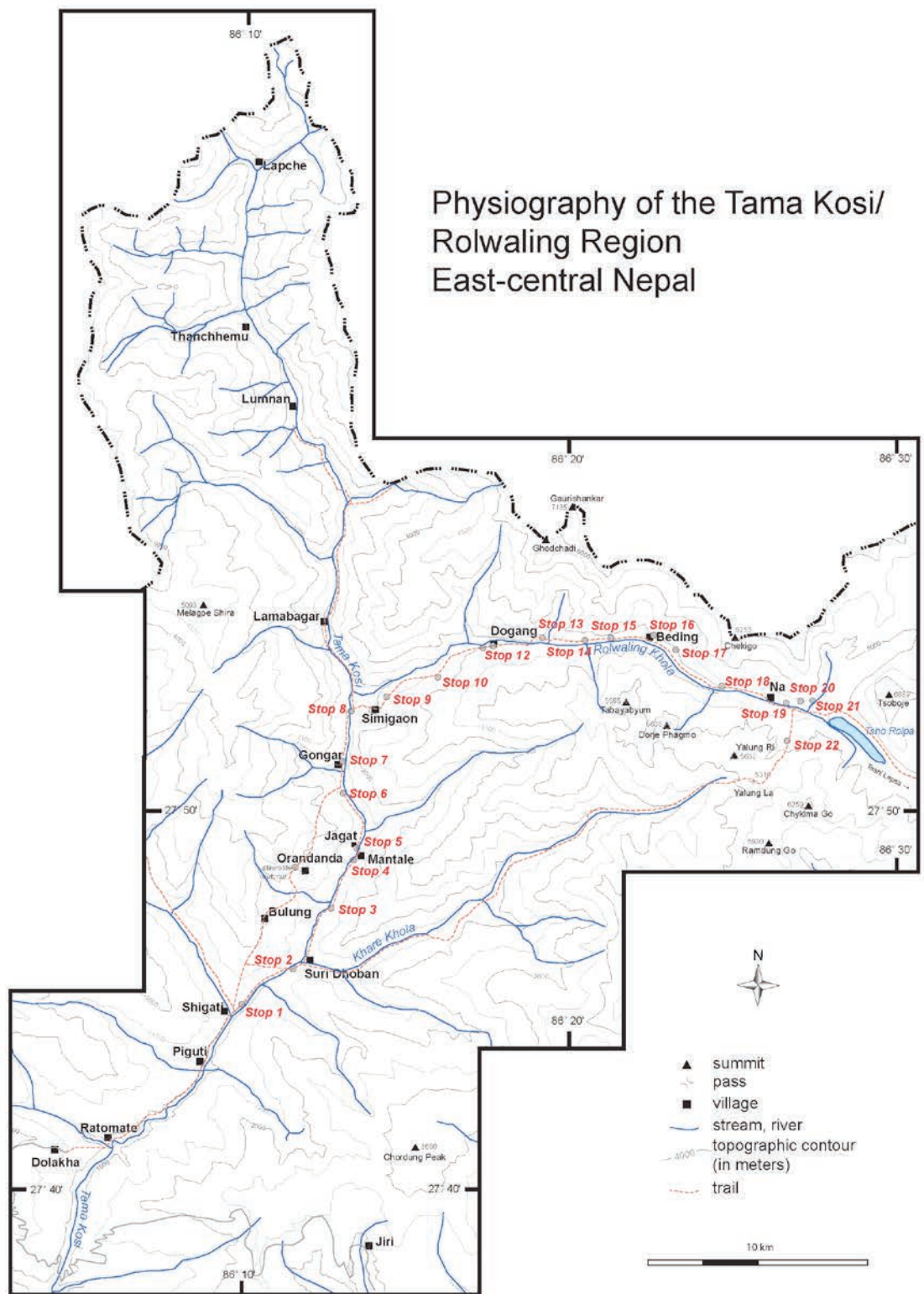


Figure 1  
 General physiographic map of the Tama Kosi/Rolwaling region. Stop locations mentioned in the text are noted. The location of this map / field trip area is shown in Figure 2.

– Carosi et al. 2010 and Montomoli et al., 2013; far west Nepal – Yakymchuck and Godin, 2012). Those that occur at a structural level similar to the one in the Tama Kosi region may mark the transition between deformation recorded in the deep hinterland and deformation recorded in the shallower foreland of the evolving orogen (e.g. Larson et al., 2010). This transect provides an opportunity to examine how convergence was accommodated at midcrustal structural levels as the Nepalese Himalaya evolved.

### Accessing the Area

Be sure to arrange all appropriate permits and logistical support in Kathmandu prior to leaving for the Rolwaling area; services are limited in the area.

Fieldwork presented in this guide was carried out in spring of 2009 and 2010. At that time the ‘end of the road’ was the town of Shigati (Figure 1). While access into the region may have changed (see below) it is recommended to begin the trip as indicated in the itinerary below to maximize examination of different rock types at various structural levels.

At the time of publication, the region is the site of a massive hydropower construction project run by Upper Tamakoshi Hydropower Limited. More information on this project is available on the company’s online site (<http://utkhpl.org.np/>). As progress on the project continues, road access, trail routes and rock exposures are subject to change. So too are potential access routes and available transportation. As a result it is possible that one or more of the outcrops presented herein along the Tama Kosi river may no longer be accessible/exposed. In such a case it would be likely that new exposure has been created, which can be examined in the context of the accompanying descriptions, and may even provide new insights. Once within the Rolwaling valley all stops and outcrops are likely to have remained unchanged.

The upper Tama Kosi and Rolwaling region can be accessed through the town of Dolakha, a ~ 4-5 hour private bus ride to the east of Kathmandu (public bus transportation would take significantly longer). At Dolakha there is an option to spend the night and then trek to the town of Shigati the next day, or take a ~2 hour bus ride from Dolakha to Shigati provided transportation (bus, jeep, tractor) can be arranged (same day is possible). For

the return trip, Dolakha is the preferred exit point for the trek as it is a major hub with easy access to multiple daily buses to Kathmandu.

### Suggested Itinerary

The trip can be completed in twelve to thirteen days. However, there are ample opportunities for side ventures along the way that can extend the time spent in the field (some will be noted below along with the potential geologic observations as appropriate). The basic itinerary is outlined in Table 1. Lodging is available in all villages indicated as ‘destinations’; however, it is advisable to be prepared to camp for a night or two depending on local vacancy as in some villages there is only one guesthouse. The farthest destination in this field guide is the village of Na in the upper Rolwaling valley (Figure 1). Na serves as a seasonal home for many of the families that typically reside in Bedding (Figure 1). It is recommended that arrangements for accommodation in Na (if desired) be made while in Bedding as, depending on the time of year, there not be anyone in Na to provide a place to stay.

The village of Na sits at an elevation of ~ 4200 m, thus participants should be prepared for possible altitude sickness. The itinerary in Table 1 typically ascends at a pace that should minimize potential symptoms of altitude sickness. It is, however, recommended that the trekker be aware of the symptoms of altitude-related problems and be prepared to descend to immediately to alleviate them. Moreover, as with any trek in the Himalaya, the participants should have a basic level of fitness that will allow them to walk for extended periods (5-8 hours) for 10+ consecutive days.

### GEOLOGIC SETTING

The Himalaya is made up of a simple series of tectonostratigraphic units that extend along much of the > 2000 km length of the mountain belt. While the basic tectonostratigraphic units may be widely recognized, the degree of variability within those units can fluctuate widely. For the purposes of this guide we will provide a broad overview of the Himalayan tectonostratigraphy, the structures that disrupt it, and the geology specific to the field trip area.

Table 1  
Suggested Itinerary.

Day <sup>1</sup>	Origin	Destination	Transportation
1	Kathmandu	Dolakha	Bus
2	Dolakha	Shigati	
3	Shigati	Jagat/Mantale	
4	Jagat/Mantale	Simigaon	
5	Simigaon	Dogang	
6	Dogang	Bedding	
7	Bedding	Na	Trekking
8	Na and Environs		
9	Na	Dogang	
10	Dogang	Jagat/Mantale	
11	Jagat/Mantale	Shigati	
12	Shigati	Dolakha	
13	Dolakha	Kathmandu	Bus

<sup>1</sup>This itinerary is suggested based on the authors' experience in the Tama Kosi and Rolwaling valleys in 2009 and 2010. Significant construction-related changes may have occurred since the gathering of this

## Geology of the Himalaya

At the orogen scale the Himalaya is made up of four fault-bounded tectonostratigraphic domains (Figure 2). The rocks in these domains are remnants of the northern India continental margin sedimentary wedge that was detached from the Indian basement and deformed during continent-continent collision.

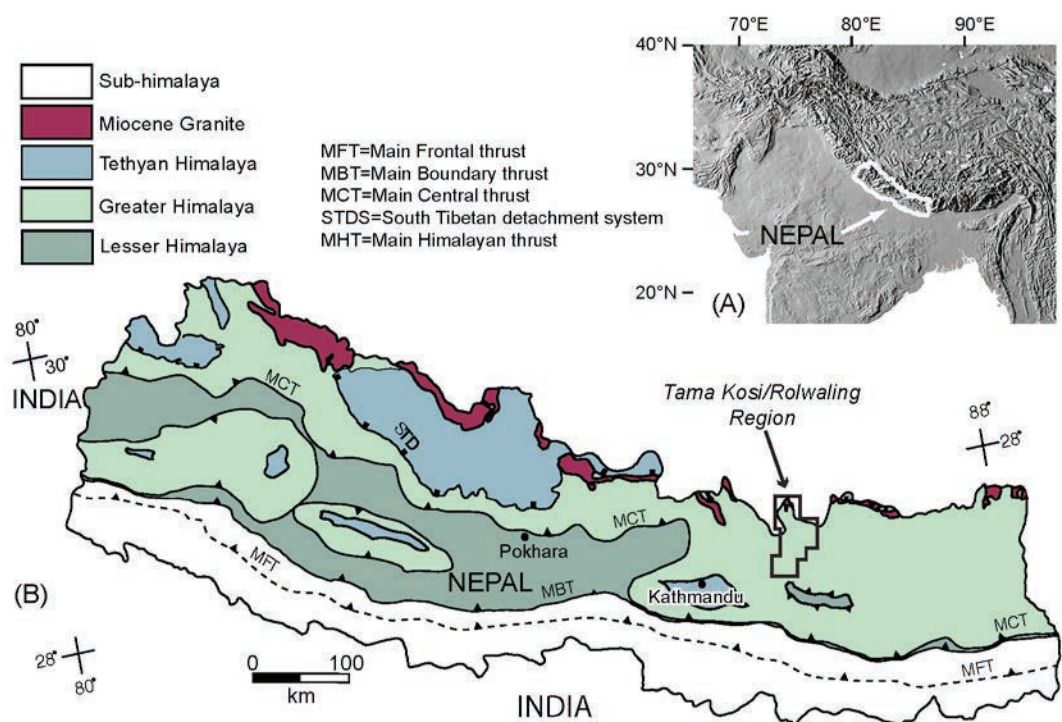
The northernmost domain is made up of unmetamorphosed-to-low-grade metasedimentary rocks (the Tethyan sedimentary sequence) (Yin, 2006) that are bounded to the north and separated from rocks of Eurasian affinity by the Indus-Tsangpo suture (Yin and Harrison, 2000). The Tethyan metasedimentary rocks are separated from the subjacent Greater Himalayan sequence to the south by the north-dipping South Tibetan detachment system. The Greater Himalayan sequence, also known as the Greater Himalayan crystallines or the Tibetan slab, is composed of upper greenschist to upper amphibolite facies paragneiss, orthogneiss, and leucogranite (e.g. Larson et al. 2010). The Greater Himalayan sequence is juxtaposed against the underlying Lesser Himalayan sequence along the north-dipping Main Central thrust (Heim and Gansser, 1939). The Lesser Himalayan sequence (sometimes referred to as the Midlands Group or, in part, as the Lesser Himalayan crystallines) is dominantly composed of an unmetamorphosed-to-low grade sedimentary succession with intercalated augen orthogneiss. The Lesser Himalayan sequence is bounded below by the north-dipping Main Boundary thrust that places the Lesser Himalayan sequence atop the Siwaliks (Yin and Harrison,

2000), the unmetamorphosed foreland deposits of the Himalayan orogen that have now been incorporated into its deforming foreland wedge. The Siwaliks are preserved in the hanging wall of the Main Frontal thrust at the leading edge of the Himalayan thrust system.

The main bounding faults of the Himalaya are all north dipping. The Main Central, Main Boundary, and Main Frontal thrusts (Figure 2) are all thrust sense structures that record top-to-the-south sense translation and young from north (Main Central thrust) to south (Main Frontal thrust). The South Tibetan detachment system, however, typically records the opposite sense of shear, top-to-the-north, and is a normal-sense stretching fault in the sense of Means (1989). The timing of movement on the South Tibetan detachment system varies both along the Himalayan orogen (Godin et al., 2006 and references therein; Kellett et al., 2013) and across related transverse structures (e.g. Kellett et al., 2009). Motion on the detachment system, however, is largely accepted to have occurred between the Early and Middle Miocene (Godin et al., 2006). This overlaps with estimates for timing of movement across the Main Central thrust, and implies that the Greater Himalayan sequence, which is bound above and below by these normal and reverse-sense faults, respectively, was extruded laterally southward during coeval movement on the two fault systems (Godin et al., 2006).

While the basic structure of the Himalaya and the tectonostratigraphic units therein are typically described in relatively simplistic terms, there is significant disagreement in how the Main Central thrust, and therefore the Greater Himalayan sequence and Lesser Himalayan sequence it juxtaposes, should be defined and identified (e.g. Martin et al., 2005; Searle et al., 2008; Larson and Godin, 2009). No broad consensus on precisely how the Main Central thrust is recognized across the Himalaya has emerged. For the purposes of this field trip we avoid distinction between the Lesser Himalayan sequence and Greater Himalayan sequence, but instead consider all rocks that record a Cenozoic metamorphic, deformational, and thermal history as parts of the Himalayan metamorphic core in the hanging wall of the Main Central thrust. Mapping the Main Central thrust at the base of Cenozoic deformation, metamorphism and thermal influence in this manner is broadly consistent with the interpretation of Searle et al. (2008). When using this field guide or comparing any investigations of the Main Central

**Figure 2**  
General geologic map of the Nepalese Himalaya. Geology modified from Martin et al. (2005); figure modified from Larson (2012). The location of the field trip area (Figures 1 and 3) is indicated.



thrust the reader should be aware of how this key structure is defined in each case.

### Research in the Tama Kosi and Rolwaling region

The Tama Kosi and Rolwaling region was first mapped at a reconnaissance scale as part of a broader mapping campaign of east-central Nepal by T. Ishida in the 1960's. Ishida eventually published two papers that included information on the geology of the region (Ishida, 1969; Ishida and Ohta, 1973). These early contributions demonstrated that all of the rocks in the region have been metamorphosed and that the general metamorphic grade increases up structural section towards the north. A later regional study by Schelling (1992), which included parts of the present study area, expanded on the initial work of Ishida and reinterpreted the rocks in terms of the contemporary organization of Himalayan geology outlined above. Schelling (1992) mapped the Main Central thrust as occurring in the middle of the present field guide area near the town of Jagat (Figures 1 and 3). This interpretation placed Greater Himalayan sequence rocks to the north of Jagat and Lesser Himalayan sequence rocks to the south.

Larson (2012) published the first detailed field lithotectonic, structural, and petrologic descrip-

tions for the area. Based on these new observations and the Searle et al. (2008) definition of the Main Central thrust, Larson (2012) mapped the fault structurally below, or south of, the present field guide region. This study was followed up by a more detailed, laboratory-based study linking metamorphic conditions to time via microstructures and variations in trace elements of dated monazite across the region (Larson et al., 2013). The study indicated the presence of a structural, metamorphic, and geochronologic discontinuity within the exhumed metamorphic rocks of the area. This discontinuity represents a tectonic juxtaposition of hanging wall rocks (metamorphosed and deformed while part of a laterally translated midcrustal layer that moved out from the orogenic hinterland) against footwall rocks that never extended in to the orogenic hinterland, but were deformed and metamorphosed during their incorporation into an evolving wedge taper along the foreland of the Himalayan orogen (Larson et al., 2013).

### Lithologies

The rocks exposed in the Tama Kosi and Rolwaling valleys include a wide range of lithologies of various metamorphic grades and local anatexite content (Larson, 2012). The rocks are dominant-

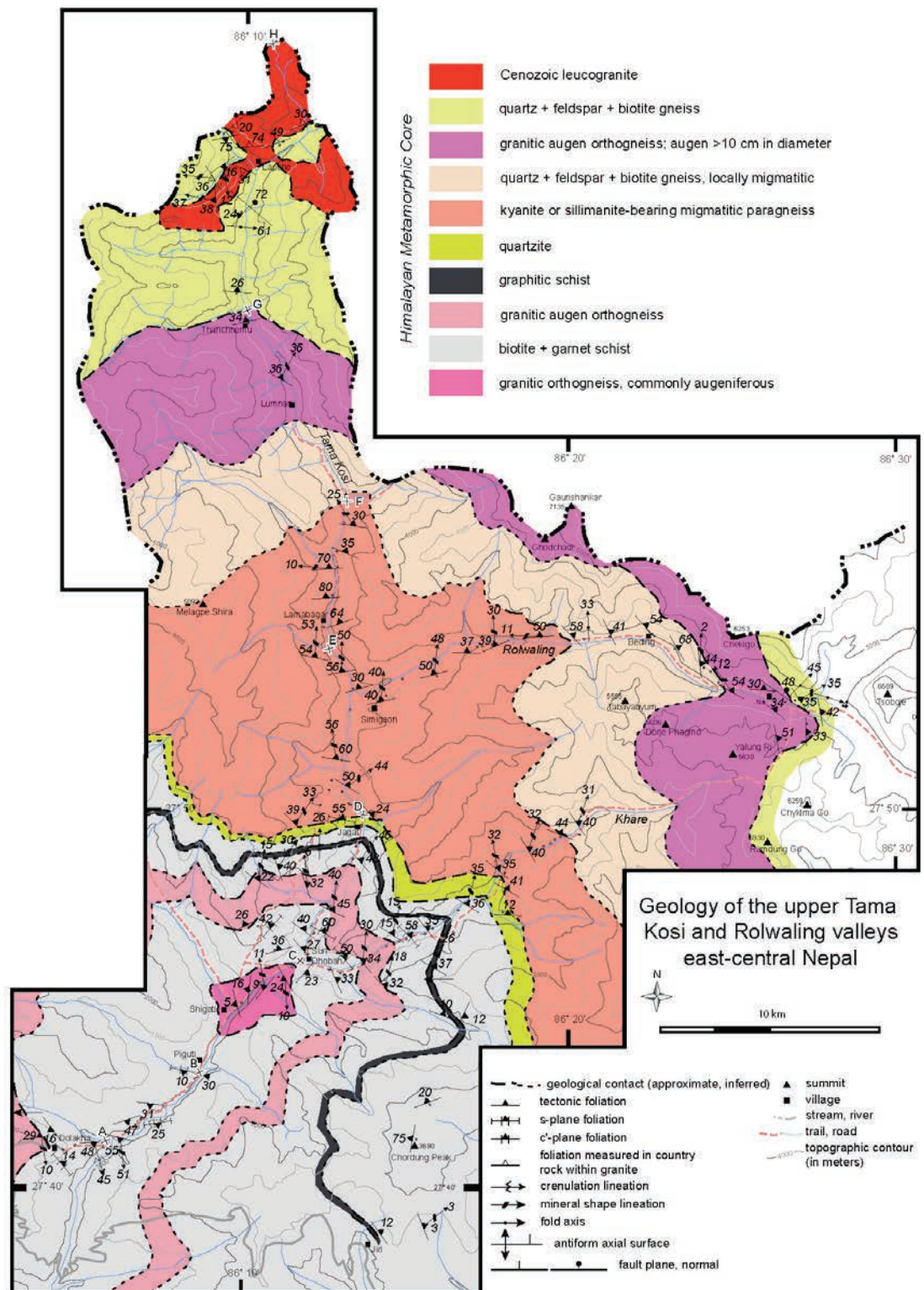


Figure 3  
Geology of the Tama Kosi/  
Rolwaling region. Map  
location shown in Figure  
2. Modified from Larson  
(2012).

ly metasedimentary but are intercalated with meta-igneous rocks at multiple structural levels (Figure 3). Both metamorphic grade and general volume of anatexite increase up structural section, from south towards the north. The structurally

lowest rocks, in the south, are at garnet-biotite grade followed by staurolite grade, kyanite grade, and finally sillimanite grade traced up structural section (Figure 4). Anatexite at the structurally lowest levels is only locally present, and where

observed comprises less than 5% of the rock by volume. The total anatexite volume is relatively low south of the village of Jagat. Just north of Jagat, anatexite comprises a significant portion of the rock volume (20-30%), while the structurally highest rocks are migmatitic and show evidence for multiple melt generating events. At sillimanite grade the rocks comprise up to 50-60% anatexite (Larson, 2012).

providing local fresh exposures of the rock in road cuts.

### Optional Stop - Dolakha (N27.68129°, E086.07209°)

If you are traveling to Shigati from Dolakha there are numerous opportunities to examine the au-

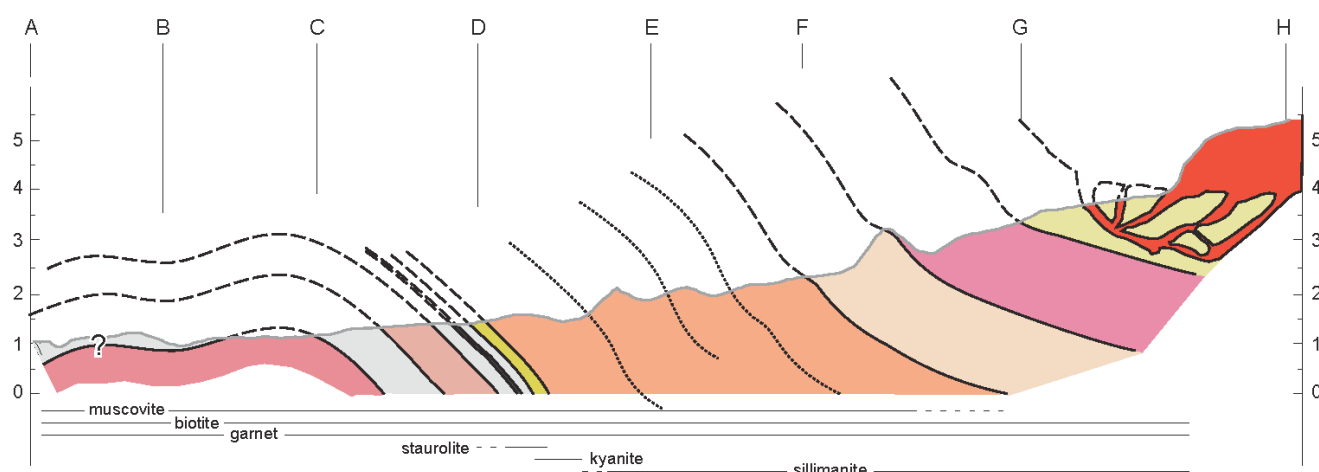


Figure 4

Generalized vertical geological section drawn across the Tama Kosi/Rolwaling region. The line of section is outlined by letters A through H on Figure 3. Modified from Larson (2012).

Table 2

X-ray Diffraction Major Element Analyses of Orthogneiss Specimens from the Tama Kosi Valley.

Specimen	Na <sub>2</sub> O	MgO	Al <sub>2</sub> O <sub>3</sub>	SiO <sub>2</sub>	P <sub>2</sub> O <sub>5</sub>	K <sub>2</sub> O	CaO	TiO <sub>2</sub>	MnO	Fe <sub>2</sub> O <sub>3</sub>	S	Sum
TK09B	2.91	0.99	14.2	65.2	0.14	5.07	0.66	0.3	0.04	3.23	<0.01	92.8
TK46	2.91	0.58	15.1	66.7	0.22	5.09	0.66	0.3	0.04	2.74	<0.01	94.3
TK54	2.77	0.56	14.7	68.3	0.23	5.21	0.56	0.28	0.05	2.84	<0.01	95.4

## FIELD GUIDE AND SUGGESTED FIELD STOPS

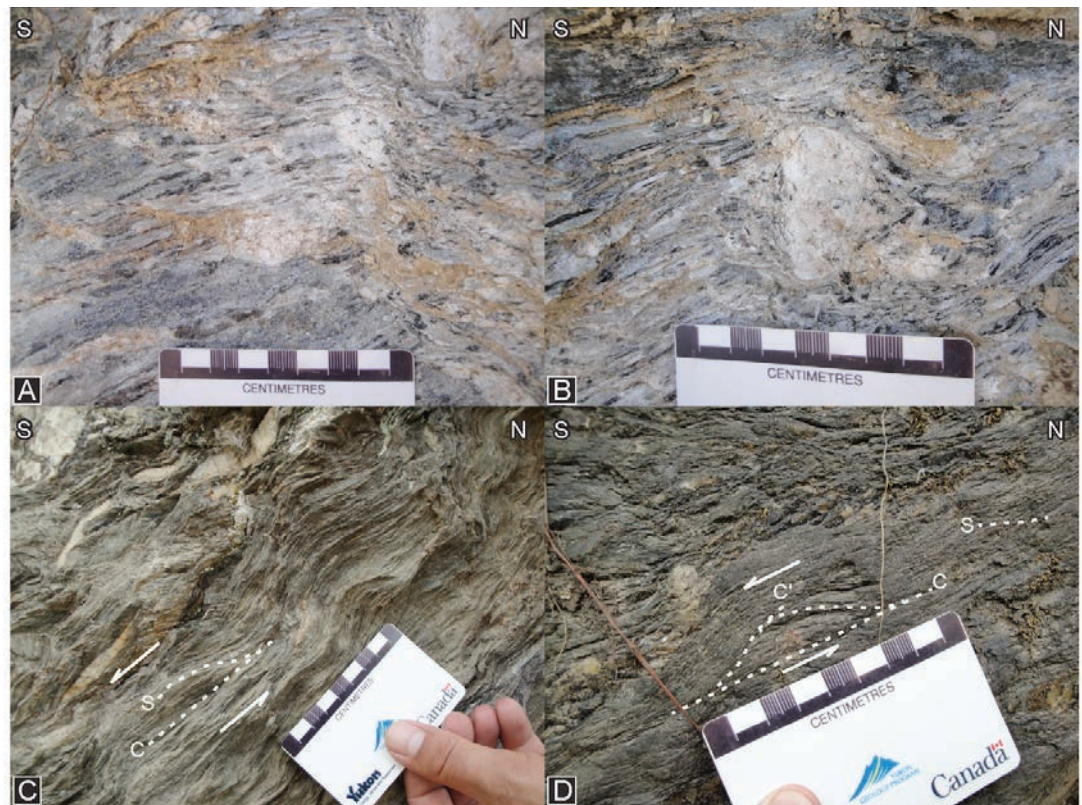
A start from Dolakha begins the field trip at a higher structural level than a start from Shigati (Figures 1 and 3). Dolakha town is built on a ridge that is capped by mylonitic augen orthogneiss (Figure 3) that is equivalent to the Melung augen gneiss of Ishida (1969) and Schelling (1992) (Table 2) and to the Ulleri and Phaplu orthogneisses elsewhere along the orogeny (Schelling, 1992). The main bus route from Dolakha to Shigati cuts progressively down section across the orthogneiss

gen orthogneiss. Relatively new exposures along the road, however, afford a unique opportunity to examine 'fresh', less weathered material. As shown in Figure 5A, fresh outcrops of the mylonitic orthogneiss are typically composed of quartz + alkali feldspar + muscovite + plagioclase + biotite. Dark biotite grains that help define the stretching lineation in hand sample (locally an L tectonite), are easily picked out against the lighter quartz and feldspar (Figure 5A). Moreover, the fresh exposure allows the recognition of local leucocratic anatexite pods that are otherwise difficult to distinguish in weathered exposures. These pods typically cross-cut the mylonitic foliation and lineation, but do record some deformation. As such they are interpreted to be late synkinematic (i.e. likely Miocene) (Figure 5B). There are as yet no direct age constraints for these anatexite pods.

Structurally below the augen gneiss, on the way to Shigati you will pass a garnet-bearing quartz + muscovite ± biotite phyllite that is locally intercalated with a fine to medium grained meta-sandstone (Larson, 2012). This lithology has yet to

Figure 5

A) Orthogneiss near the town of Dolakha. B) Leucogranite pod within the same orthogneiss shown in A. C) Planar fabric elements indicated top-to-the-south shear in phyllitic schist. D) Planar fabric elements indicated top-to-the-south shear in phyllitic schist.



yield any thermobarometric data and no useful chronometers such as zircon, monazite and apatite have yet been found. The only potentially useable mineral for U-(Th)/Pb geochronology found was allanite, but major problems with common Pb contamination prevented extracting meaningful age data. The phyllite does, however, have planar deformational fabrics such as S, C, and C' structures (Figures 5C, D). These fabrics typically define a top-to-the-south sense of shear (Larson, 2012).

### Day One - Lower portion of the exhumed metamorphic core

The rocks traversed in this section comprise part of the Midland Group of Ishida (1969) and are here interpreted here as the lower part of the Himalayan metamorphic core. The rocks traversed on Day 1 record synkinematic metamorphism along a burial path during the Middle Miocene (Larson et al. 2013).

Stop 1 - North of Shitagi  
(N27.73971°, E086.16861°)

Shitagi village is located at approximately the low-

est structural position described in this field guide. The area around the town, and as far north as the village of Suri Doban (Figure 3), is underlain by orthogneiss termed the Suri Doban orthogneiss by Ishida and Ohta (1973) and Schelling (1992). The Suri Doban orthogneiss is locally an augen gneiss, but is more commonly fine-to-medium grained with quartz + alkali feldspar + plagioclase + muscovite + biotite ± chlorite with accessory apatite and epidote. Preliminary geochemical analyses (discussed in Stop 3 below) confirm the mineralogical differences and unique structural position of the Suri Doban orthogneiss relative to the structurally higher Melung orthogneiss.

The orthogneiss at the listed stop location is fine-to-medium grained and augen are absent. Locally preserved small (cm-scale) augen can be observed in outcrops exposed farther north along the trail, though they are measurably smaller and less abundant than augen of the Melung orthogneiss. At the stop location, which, unfortunately, may be hidden behind a rock bail wall now, but was still accessible in 2010, the orthogneiss is intruded by a leucogranite dyke (Figures 6A, B). The leucogranite dyke is generally discordant to the main foliation, though it does show evidence of shear sub-parallel to the foliation plane (Figure 6C). Moreover, the dyke has a dark fine-grained

Figure 6

A) Deformed leucogranite dyke (white colored rock) cutting orthogneiss. People for scale. B) Deformed leucogranite dyke within orthogneiss. C) Close-up photograph of the margin of the leucogranite dyke with the orthogneiss. D) Variably disaggregated, stromatic leucogranite in schistose rocks (from Larson, 2012). E) Apparent compositional layering in quartzite. F) Leucogranite within biotite-rich schist; hammer is 36 cm long. G) Leucogranite lens with biotite-rich rims in quartz + biotite schist (from Larson, 2012)



rind (Figure 6C), the nature of which could be related to differential shearing and strain localization, localized contact metamorphism, or, perhaps, marks a melanosome in which case the dyke

indicates in situ partial melting. It is not known if this leucogranite is related to the leucogranite pods noted in section 3.1 within the Melung augen orthogneiss.

### Stop 2 – North of Suri Doban (N27.75690°, E086.193320°)

The area around Shigati is underlain by the Suri Doban orthogneiss and represents the core of a structural culmination located in the southern part of the map area along the Tama Kosi river (Figure 3). To the north, near Suri Doban, the effects of this structural culmination are no longer reflected in the orientation of the dominant tectonic fabric; almost all foliations now dip to the north (Figure 3).

This stop is to visit an outcrop of phyllite that separates the two orthogneiss units. As discussed above, the phyllite is intercalated with meta-sandstone lenses. The meta-sandstone at this site is unique in that it is a relatively pure quartzite, whereas most lenses are more typically arkosic. C/S/C' fabrics are visible in outcrop and continue to define a top-to-the-south sense shear.

### Stop 3 – Melung Augen Orthogneiss (N27.78451°, E086.21161°)

Those who chose to start their trip in Dolakha should find the rocks in this outcrop familiar, as this is the same quartz + alkali feldspar + muscovite + plagioclase + biotite augen orthogneiss horizon of Melung augen orthogneiss that can be followed southward to the town of Dolakha. The alkali feldspar augen in this outcrop are particularly large and act as winged porphyroclasts further confirming the top-to-the-south shear sense indicated by the C/S/C' fabrics observed structurally below.

Whole rock geochemical analyses (Table 3) further differentiate between the Melung and Suri Doban orthogneiss units. The percent oxide values presented in Table 3 were obtained through loose powder X-ray diffraction analyses. Specimen TK09B was sampled from the structurally lower Suri Doban orthogneiss while specimens TK46 and 54 were taken from the Melung augen gneiss. Mg and Fe oxides in the Suri Doban specimen are significantly lower than those from the Melung specimens (Table 3). As well, the Al and P oxides for the Suri Doban specimen are significantly lower than those in the Melung specimens.

Quartz lattice preferred orientation at a slightly higher structural level within this orthogneiss defines an asymmetric crossed girdle fabric (Figure 7A; specimen TK-46) that supports the overall top-to-the-south shear sense noted at the outcrop scale. Furthermore, the opening angle of the fab-

ric measured across the foliation pole indicates that plastic deformation recorded in the recrystallized quartz grains occurred at  $\sim 625 \pm 50$  °C (Figure 7D; Larson et al., 2013).

### Stop 4 – Phyllitic Schist (N27.807603°, E086.224828°)

*NOTE – The latitude and longitude values for Stop 4 are approximate as they are derived from a best-approximation, plotted position of this outcrop on a trekking map.*

From the previous stop (3) to this one, the bedrock is dominated by the Melung orthogneiss with rare intercalations of metasedimentary rocks. The orthogneiss gives way up structural section to phyllitic schist and schistose phyllite. These metapelitic rocks are well-foliated and retain evidence of transposed compositional layering. They also host partially disaggregated, plastically deformed quartz-rich dykes or veins (Figure 6D). An outcrop from a similar structural level on the ridge located on the west side of the river contains staurolite porphyroblasts (Figure 1; co-ordinates are provided below). One specimen from that outcrop (TK45) has been analysed using isochemical phase equilibria modeling and yields a peak temperature between  $\sim 610$ - $650$  °C at a pressure between 625 and 700 MPa (Larson et al., 2013). These results are consistent with nearby estimated deformation temperatures (see previous stop) indicating that deformation was likely coeval with near peak metamorphism, an interpretation supported by the synkinematic microstructure of the staurolite porphyroclasts (Larson et al., 2013). Furthermore, monazite grains from both the matrix and within staurolite grains yield ages ranging between c. 10 and 8 Ma, which indicates that metamorphism and deformation occurred in the Late Miocene. The pressure-temperature-time path interpreted for these rocks is consistent with paths modeled for the foreland part of a deforming orogenic wedge (Figure 8A; Larson et al., 2013). This is compatible with recent studies that interpret the lower portions of the exhumed Himalayan mid-crust as having been deformed and metamorphosed primarily as part of a foreland thrust wedge (e.g. Larson et al., 2010; Yakumchuk and Godin, 2012; Larson et al., 2013).

On the way back at the end of this trek it is possible to follow a trail from near Gongar up onto the ridge towards the town of Bulung (Figure 1). Doing so would allow a visit to the staurolite

Table 3  
Tectonostratigraphy Comparison

Schelling (1992)		Ishida (1969) and Ishida and Ohta (1973)			
HIGHER HIMALAYAN CRYSTALLINES	Main Central thrust	<i>Rowaling-Khumbu granites</i>	<i>Khumbu formation</i>	<i>Khumbu thrust</i>	HIMALAYAN GNEISSES
		<i>Rowaling-Khumbu paragneiss</i>			
		<i>Rowaling-Khumbu migmatite</i>	<i>Solo formation</i>	<i>Solo thrust</i>	
		<i>Junbesi paragneiss</i>			
LESSER HIMALAYAN SERIES		<i>Khare phyllite</i>	<i>Jiri formation</i>	<i>Jiri thrust</i>	MIDLAND METASEDIMENT GROUP
		<i>Melung-Salleri augen gneiss</i>			
		<i>Dolakha phyllite</i>	<i>Melung augen gneiss</i>	<i>Midland thrust</i>	
		<i>Suri Dhoban augen gneiss</i>	<i>Dolakha formation</i>		
		<i>Tam(b)a Kosi window formation</i>			

modified from Larson (2012)

lite-bearing outcrop (N27.79786°, E086.19167°) for which the pseudosection was developed, as well as a visit to an outcrop of a graphitic schist unit (N27.80990°, E086.20252°) that is noted elsewhere in the region, but does not crop out along the river (Larson, 2012).

#### *Jagat/Manthale – A Structural Discontinuity*

The towns of Jagat and Manthale span a major river crossing and mark one of the most interesting features in the geology of the region. South of the towns the rocks are staurolite grade and lower, with little anatexite. North of the towns the rocks are kyanite grade and higher, and typically contain ≥15 % anatexite by volume. The change in character of the rock, which occurs approximately at Manthale/Jagat, marks the location of a major discontinuity. Rocks below the discontinuity generally record Late Miocene synkinematic metamorphism with characteristics consistent with a burial path typical of those formed in a foreland thrust wedge (see Stop 4; Larson et al., 2013). In contrast, the kyanite and higher-grade rocks above record a protracted Early to Middle Miocene metamorphic history (to be discussed at upcoming stops) and display characteristics consistent with lateral mid-crustal flow processes (e.g. Beaumont et al., 2001; Jamieson et al., 2004). For a detailed discussion of the discontinuity see Larson et al. (2013) and references therein.

## Day Two

On this day one follows the river from Manthale/Jagat northward into the hanging wall of the discontinuity described above. The trek does not cover much horizontal ground today, but finishes with a sustained ascent to the town of Simigaon.

### Stop 5 – Quartzite (N27.81643°, E086.22607°)

This outcrop is located within the town of Manthale/Jagat on the west side of the river; it is a slab of quartzite on the trailside. The rock here is a light to medium grey-weathering quartzite sparsely intercalated with phyllitic schist. Thin biotite partings in the quartzite help mark a moderately northeast dipping foliation plane (Figure 6E). The quartzite forms a useful marker unit that can be traced across a number of valleys in the region (Figure 3) and appears to extend into adjacent drainages (From and Larson, in press). Little evidence of anatexite is recorded in these rocks, likely a function of the relatively infertile protolith.

Aluminosilicate minerals first appear north of this outcrop as the trail leads up structural section. Keep an eye on the outcrops as you travel to the next stop. Generally, the aluminosilicates first appear in close association with leucogranite pods.

### Stop 6 – Leucosome-bearing Biotite-rich Schist (N27.88638°, E086.21870°)

Recent roadwork has revealed a fresh exposure of biotite-rich schist with abundant leucocratic material (Figure 6F). This leucocratic material, which comprises a significant volume of the overall rock, may be disaggregated anatexite reflecting in-situ partial melting. Such an interpretation is supported by the presence of a biotite-rich residuum around larger leucosome lenses (Figure 6G). The anatexite pods appear to behave as semi-rigid porphyroclasts and record a dominant top-to-the-south sense shear. This shear sense is confirmed by the asymmetry of secondary foliation planes (C/S/C') within the schist itself.

### Stop 7 – Kyanite schistose gneiss (N27.85055°, E086.21867°)

The specimens collected from this outcrop (Figure 9A) have been subject to phase equilibria

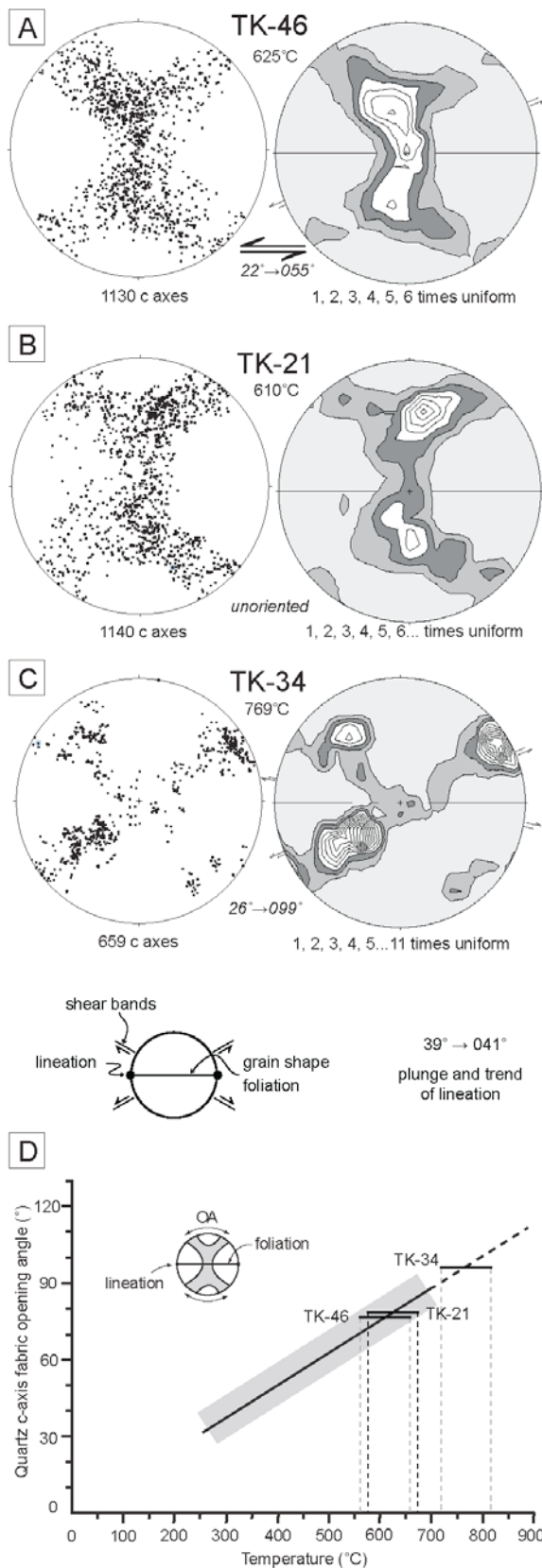


Figure 7

A-C) Quartz crystallographic preferred orientation fabrics for specimens from the field area from low to high structural levels. See text for discussion. Deformation temperature is shown with the fabrics as derived from the graph in D (modified from Morgan and Law, 2004)

modeling, in situ U-Th-Pb monazite dating, quartz petrofabric analyses, and are currently being processed for 40Ar/39Ar analyses. The rock here is a kyanite + biotite + garnet + muscovite pelitic schistose gneiss. It records a clockwise pressure-temperature-time-deformation (P-T-t-D) path that includes peak pressure conditions of 970 – 1050 MPa associated with temperatures of ~700-725 °C (Larson et al., 2013). These conditions were reached between c. 23 and 19 Ma immediately after which the rock records decompressional heating leading to the breakdown of garnet and the growth of kyanite at c. 18 Ma (Larson et al., 2013). Younger monazite age data are consistent with further decompression and significant anatexis (Figure 9B) until c. 15 Ma. Quartz lattice preferred orientation data from this outcrop (Figure 7B) indicate that deformation took place at a temperature of 610 ± 50 °C (Figure 7D; Larson et al., 2013). C/S/C' fabrics recorded in outcrop indicate that deformation was associated with a top-to-the-south shear sense (Figure 5E of Larson, 2012; Figure 9B). The 610 ± 50 °C deformation temperature estimated from quartz c-axis fabric opening angle data is significantly lower than the calculated metamorphic temperatures. This indicates that the deformation recorded occurred after peak metamorphism along the cooling path and likely in the subsolidus after c.15 Ma. The P-T-t-D path derived from this outcrop fits well with model paths from thermo-mechanical simulations of lateral midcrustal flow within the Himalaya (Figure 8B; Larson et al., 2013). This is consistent with the interpretation of a tectono-metamorphic discontinuity separating these rocks from those structurally lower in the section.

Stop 8 – Sillimanite schistose gneiss (N27.87187°, E086.22228°)

The quality of the outcrop at the specified coordinates is poor. However, you will encounter similar rocks as you work your way up the staircase (Figure 9C) leading to Simigaon – the rest stop for the day – so it is useful to describe them at the present location. The stop also acts as a crossroads where

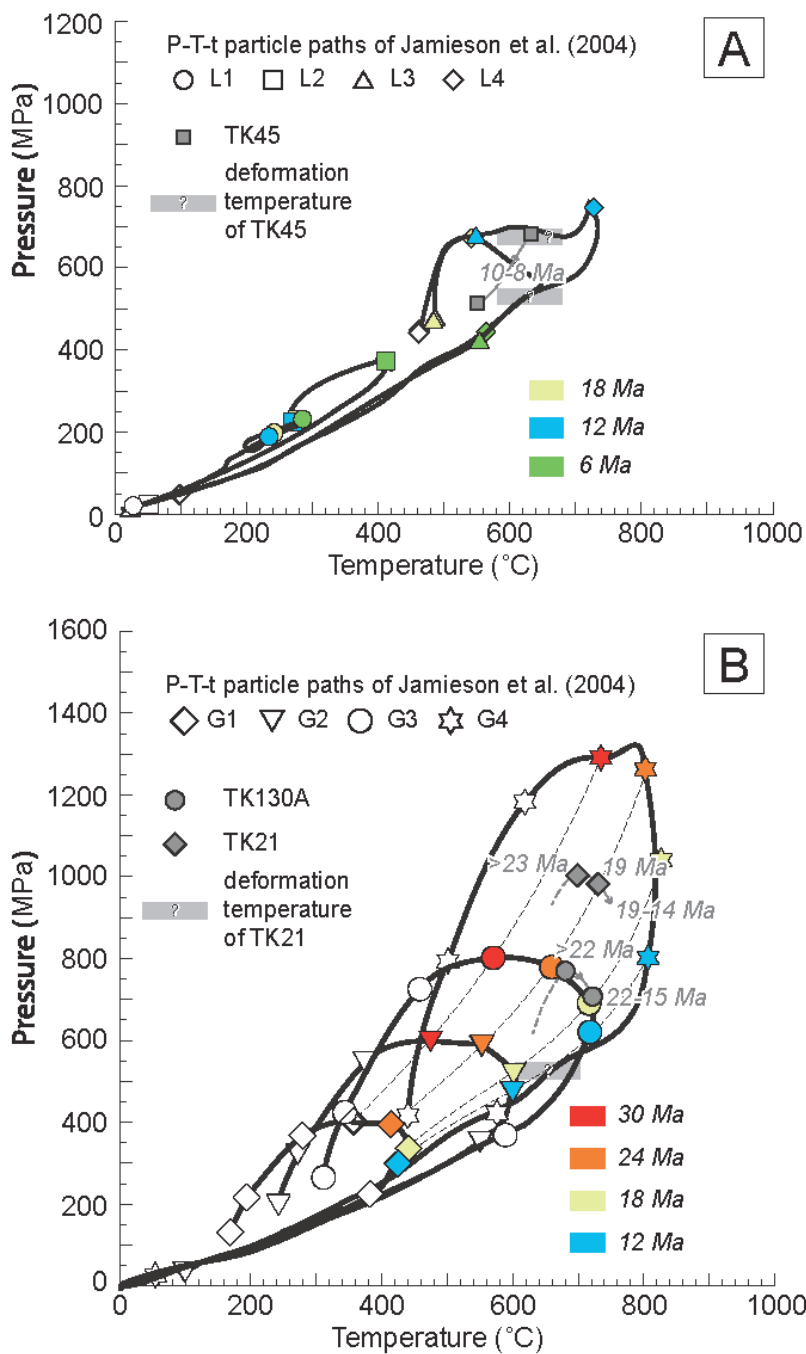


**Figure 8**  
Interpreted pressure – temperature – time paths for rocks collected below major discontinuity (A) and above major discontinuity (B). Modified from Larson et al. (2013). See text for discussion.

the trail diverges in two directions. One leads up and to the east into the Rolwaling valley while the other leads up and to the north, following the Tama Kosi valley up to the town of Lamabagar

and beyond to its head wall. The trail north used to be a precipitous journey with traditional Nepali bridges and walkways precariously clinging to cliff-sides (Figure 9D and E). Now, however, if you wish to head north you can follow the road that has been carved out of the mountainside (Figure 9F).

The rock at this stop and on the climb to Simigaon is dominantly sillimanite + biotite + garnet + muscovite-bearing migmatitic paragneiss; leucosome comprises a significant volume of the rock. Foliation is defined by preferred orientation of mica in the rock and strataform leucosomal layering, while macroscopic lineation is often marked by aligned sillimanite and muscovite grains. Where present, shear sense indicators in these rocks continue to indicate a top-to-the-south shear sense.

*Simigaon*

Simigaon is an idyllic village located on the apex of a ridge high above the confluence of the Tama Kosi and Rolwaling rivers (Figure 10A). The views from Simigaon are excellent and on clear days the high Himalaya can be seen (Figure 10B). Moreover, a view up the Tama Kosi valley to the north toward the village of Lamabagar shows that the flood plain the village is built atop was created when the Tama Kosi valley was blocked by a large landslide (Figure 10C). From Simigaon this trek now leaves the Tama Kosi valley and begins an almost west-to-east transect across the high-grade metamorphic core of the orogen through the Rolwaling valley. The dominant orientations of the tectonic foliation and unit contacts also rotate slightly such that we continue to walk largely oblique to strike (Figure 3).

**Day Three**

The trek today involves a fair amount of hiking along well-worn paths through forest. As a result, outcrop is limited. The rocks that have been examined on this stretch of the trek, however, have provided key constraints on the metamorphic and geochronologic history of the area.

**Stop 9 - Sillimanite migmatitic schistose gneiss - (N27.88244°, E086.23951°)**

The first stop exposes similar rocks to those ob-



Figure 9

A) Abundant leucogranite (white lenses) within the high-grade rocks. B) Leucogranite and associated biotite-rich residuum (hammer is 36 cm long). C) The staircase leading up to Simigaon as viewed from the west side of the Tama Kosi valley. D) A local bridge spanning part of the Rolwaling River near its confluence with the Tama Kosi. E) Cliffs with a trail network across it visible near the base. F) Construction of the road on the west side of the Tama Kosi valley leading toward Lamabagar.

Figure 10

A) The village of Simigaon. B) Gauri Shankar Himal. C) View towards Lamabagar from the south. The village is built on landslide deposits that filled the valley floor. D) Late anatexite cross-cutting foliation (from Larson, 2012). E) Cordierite (green mineral) within late anatexite. F) Pegmatitic muscovite booklet within late anatexite.



served at the base of the hill beneath Simigaon (Stop 8), though at a different structural level. The rocks in this outcrop comprise sillimanite + garnet + biotite + muscovite schistose gneiss with stratiform anatectite lenses of feldspar + quartz + muscovite. A poorly defined  $C/S/C'$  fabric can be observed in mica-rich horizons and generally indicates a top to the south shear sense.

**Stop 10 - Sillimanite migmatitic schistose gneiss -** (N27.88809°, E086.26345°)

The lithology at this stop is similar to that of Stop

9. This is a migmatitic sillimanite-bearing schistose gneiss. The material from this outcrop has been subjected to in-situ monazite dating, which has provided some insight into the metamorphic and anatectic history of these rocks. Moreover, rocks from approximately the same structural level farther to the north in the Tama Kosi valley have been used to generate a phase equilibria model that has helped constrain the pressure-temperature path of these sillimanite-bearing rocks (specimen TK130A in Figure 8B).

The pseudosection analysis yields a clockwise pressure-temperature path with peak pressures

reached prior to peak temperatures (see Figure 6 of Larson et al., 2013). The equilibrium assemblage is consistent with pressures of 710 - 770 MPa and temperatures of 720 - 750 °C (Larson et al., 2013). In situ monazite work indicates that this equilibrium assemblage likely developed at c. 22 Ma, while pressure-temperature paths indicate a

subsequent decompressional heating trajectory until c. 15 Ma (Larson et al., 2013).

The overall shape of the pressure-temperature paths and the timing constraints on the paths are consistent with those observed in the rocks at Stop 7 (Figure 8B). The P-T-t paths match well with those modeled for lateral midcrustal flow in the

**Figure 11**

A) Asymmetric leucogranite pod. B) Different leucogranite phases visible in a washed outcrop. An older, foliation parallel and a younger crosscutting phase are visible. Book is 11 cm across. C) The hamlet of Dongang. D) Migmatitic gneiss. E) Gauri Shankar.



thermo-mechanical simulations of Jamieson et al. (2004) (Figure 8B). While the P-T-t paths are not able to uniquely identify the tectonic process responsible for their formation, other evidence such as kinematic indicators and timing constraints are consistent with these rocks having been subjected to ductile lateral flow.

#### Stop 11 - Multiple leucogranite phases (N27.89742°, E086.27298°)

The rock at this stop may not be entirely 'in place'; however, it has not moved far from its source. The lithology is more gneissic in character than the previous stops of today, but maintains a similar mineral assemblage. The nature of the anatexite, however, presents some new observations; two phases of leucogranite are now present. There is an early, largely stratiform, phase similar to that observed at stop 9. It consists of feldspar + quartz + muscovite and is notably deformed along with the bulk of the rock. The second phase is younger and occurs as discrete pods that cut across the main tectonic fabric and older leucogranite phase (Figure 10D). The younger phase is typically pegmatitic in nature with large feldspar and quartz crystals and muscovite booklets (Figure 10E). Moreover, the pegmatitic younger phase locally contains cordierite crystals (Figure 10F), a mineral association common with later phase leucogranite in the Himalaya (e.g. Searle et al., 2010; Streule et al., 2010; Groppo et al., 2012; Searle, 2013). The pegmatitic leucogranite phase may be related to a large leucogranite pluton of similar character that occurs structurally higher, observed at the headwall of the Tama Kosi valley (Larson 2012). Crosscutting dykes that are potentially related to that pluton will be visited at the structurally highest point on this trek.

#### Stop 12 – Water-polished exposure of leucogranite relationships (N27.90151°, E086.28535°)

The rocks in this outcrop provide an opportunity to observe relationships between the leucogranite phases and the tectonic foliation. The outcrop has been washed clean by the stream moving over it. This provides good exposure, but can make things slippery; be careful. The lithology is similar to the previous outcrop, with multiple leucogranite generations are preserved. An earlier deformed leucogranite phase defines a local top-to-the-west

shear sense (Figure 11A), while a younger phase variably crosscuts the main foliation (Figure 11B). These rocks have demonstrably undergone multiple episodes of partial melting.

#### Dogang - (N27.90402°, E086.28801°)

The destination for today is the riverside gathering of houses known locally as Dogang (or Dognag). There is a nice area that can be used for camping (Figure 11C) and a well-constructed outhouse for use by trekkers. If the river is low enough, it is possible to hop across the stones to examine the rocks on the far side; however, they are quite similar to those that have been examined for most of the day. Tomorrow the ascent up to the village of Bedding will commence, which, at an altitude of ~3600 m, is high enough for some to begin to feel the effects of high altitude. Be aware of the possible symptoms and treatment of altitude sickness.

### DAY FOUR

On day four the trail works its way ever higher and the hike ends above the main tree-line at the town of Bedding, a welcoming, well-organized, typical Sherpa village. One of the main sources of income for the families of Bedding is high-altitude guiding and carrying for climbing expeditions to the >8000 m peaks across Nepal. Bedding boasts the most Everest summiters per capita of any village in Nepal. While staying in Bedding it may be prudent to inquire about accommodation or camping in Na. Na is a seasonal village, used mainly during the hot months and for animal grazing. Depending on the timing of your trip there may be no place to stay if you show up in Na unannounced; it is best to check in Bedding first.

The path today begins along the river valley, which is filled with colluvium, resulting in long stretches between outcrops.

#### Stop 13 - Sillimanite migmatite (N27.90391°, E086.31406°)

This first outcrop of the day exposes sillimanite-bearing migmatite with foliation parallel, deformed leucogranite (Figure 11D). The migmatite includes quartz + feldspar + muscovite + biotite ± sillimanite ± garnet, while the leucogranite lenses comprise quartz + feldspar + muscovite ± tourmaline ± sillimanite. Though the age relation-

**Figure 12**

A) Variably migmatitic, metapsammitic gneiss. B) Folding (?) within quartzite. See text for discussion. C) Recumbent folding within migmatitic gneiss. Hammer is 36 cm long. D) View up the Rolwaling valley to the east. E) Yaks in the middle of a heavy snowfall in the village of Na. F) View down the Rolwaling valley (to the west) at incoming weather.



ship between the leucogranite lenses and the leucosome within the migmatite is not particularly clear, it appears that the leucogranite lenses are the younger phase, with the foliation of the migmatite wrapping around them (Figure 11D). Unlike the younger intrusive phase observed at stop 11, however, these leucogranite lenses appear to be concordant with the main tectonic foliation.

Just up the trail from this outcrop are some of the best views of Gauri Shankar, one of the highest peaks in the region at 7135 m, to the north (Figure 11E).

#### Stop 14 - Variable Psammitic Gneiss and Quartzite (N27.90374°, E086.33268°)

The lithology at this point has changed from a metapelitic-dominated migmatite to a metapsammitic gneiss. This change is accompanied by a reduction in the amount of anatexite, or leucosome, within the rock. The rocks at this outcrop include quartzite, psammitic gneiss and paragneiss, all with varying degrees of migmatization (Figure 12A). The rocks nearby up the trail are similarly variable, however, the outcrops show some of the deformational structures within these units.

One of these structures includes a possible fold within quartzite (Figure 12B). This may reflect evidence of drag folding along a minor shear within the unit, or perhaps deformed original cross bedding. In addition, a bit farther up the trail there is a reclined fold within intercalated metapsammite and more mica-rich paragneiss (Figure 12C). Although the individual fold limbs are at an angle to the main foliation attitude, the overall shape of the fold approaches isoclinal, with an axial plane parallel to the main foliation. The fold is indicative of deformation characterized by horizontal extension and vertical thinning.

#### Stop 15 - Variable Paragneiss and Leucogranite (N27.90401°, E086.34673°)

The final stop of the day before reaching Bedding is at an outcrop that contains at least three distinct lithologies: 1) quartz + biotite metasandstone/quartzite; 2) quartz + biotite + muscovite + sillimanite + feldspar ± garnet migmatite; and 3) quartz + feldspar + biotite + sillimanite psammitic gneiss. The foliation in these rocks dips northeast, reflecting the rotation of the main foliation that is occurs along the Rolwaling.

Quartz lattice preferred orientation analysis of a quartz-rich specimen from this location reveals a c-axis fabric pattern dominated by prism [c] slip with lesser components of prism <a> (Figure 7C). The opening angle of the fabric indicates deformation temperatures exceeded 750 °C, suggesting deformation may have been coeval with near-peak metamorphism or at least occurred shortly thereafter.

#### Bedding

On the walk up the hill to Bedding you may have noticed float with ellipsoidal leucocratic nodules, presumably originating from the surrounding rock. These nodules are interpreted as faserkiesel; knots or pods of quartz + sillimanite ± muscovite ± K-feldspar. The formation of faserkiesel appears to be compositionally dependent and may reflect a former stable K-feldspar + sillimanite assemblage that has been subject to retrograde metamorphism involving paired ionic equilibria (Tippet, 1984). If that interpretation is correct it implies that the mineral assemblage preserved in the sillimanite grade rocks does not represent peak metamorphic conditions. More detailed phase equilibria modeling of these rocks is being

carried out to investigate this possibility.

#### Day Five

Today is a short trek day necessitated by the climb in elevation to the destination of Na. There is much rock to examine along the way, though much of it crops out some distance off of the main trail. The landscape and minimal cover in the area makes it relatively easy to reach those outcrops.

It is worthwhile mentioning that you are now in an alpine environment in which the weather can change drastically and quickly (Figure 12D). One year on traverse we were caught in a four-day snowstorm (Figures 12E and F) and were forced to retreat back down to lower elevations through thigh-deep snow. Be prepared for any and all potential weather conditions.

#### Stop 16 – Quartzo-feldspathic gneiss (N27.90411°, E086.37676°)

The first stop today is to look at the outcrops just above the town of Bedding. The rocks here are similar to the rocks examined towards the end of the Day 5 (yesterday), with abundant quartzo-feldspathic gneiss intercalated with more mica-rich layers. You will likely notice, on your walk up to the outcrop, that there is abundant float with large K-feldspar crystals; we will examine the source rocks tomorrow. Be sure to explore the outcrop as the lithology, structural style, and relationship between the country rock and leucogranite can vary locally. The main lithology appears to be a meta-sandstone (Figure 13A) that contains course-grained to pegmatitic quartz + feldspar + tourmaline ± muscovite leucogranite lenses. This leucogranite follows the foliation locally (Figure 13A), but is also seen cutting across the foliation at a high angle (Figure 13B) indicating it may be late syn-to-post kinematic.

Isoclinal folding (Figure 13C) similar to that observed below indicates horizontal stretching and vertical thinning – style deformation.

#### Stop 17 – Migmatitic Quartzo-feldspathic gneiss (N27.89985°, E086.38164°)

The rocks at this stop show the same relationship to those observed above Bedding. The main lithology exposed is quartzo-feldspathic gneiss, perhaps a meta-sandstone, with layer-parallel leu-

cosome and melanosome. The rock is cut by later, discordant, coarse-grained to pegmatitic leucogranite pods. Again, isoclinal folding of the foliation is common, with the fold axial plane parallel to the dominant foliation.

**Stop 18 –Orthogneiss contact**  
(N27.88344°, E086.40418°)

This is the approximate location of the contact between the quartzo-feldspathic paragneiss (meta-sandstone) and the structurally overlying granitic orthogneiss. Structurally higher the rocks comprise migmatitic orthogneiss in which disaggregated leucosome, or perhaps synkinematic injected dykes and/or sills, now form both foliation parallel layers (Figure 13D) and local porphyro-

clasts (Figure 13E). The orthogneiss consists of feldspar + quartz + biotite, while the leucogranite comprises feldspar + quartz + tourmaline ± muscovite. While this location represents the approximate transition between the different units, the orthogneiss observed here is not particularly typical of the majority of that unit that we will examine in future stops.

*Na*

The village of Na is a well-constructed labyrinth of stone fences and stone houses. It serves as the grazing land and summer home for many of the families in Bedding. Na sits at an elevation of ~4200 m and as such it is not a bad idea to have a rest or break here to help acclimatize to the alti-

**Figure 13**

A) Metasandstone paragneiss with abundant leucogranite lenses. B) Leucogranite dyke cross-cutting the dominant tectonic foliation. Hammer is 36 cm long. C) Recumbent folding within migmatitic gneiss. Orthogneiss with layer parallel leucosome (D) and local porphyroclasts of potentially disaggregated leucosome (E).



tude. Na will serve as the base for the next day of the field trip, which will be spent exploring farther up the valley before returning to the village at the end of the day.

### Day Six

Today will be spent exploring a region up the valley east of Na leading to the foot of Tso Rolpa, one of the largest glacial lakes in the world. Tso Rolpa is continuously monitored for potential glacial lake outburst floods (GLOFs); or at least monitoring equipment was installed. The aim of the monitoring program is to notify villagers in Bedding to move to higher ground should a flood occur.

#### Stop 19 – Augen Orthogneiss - (N27.87855°, E086.43808°)

At this location the orthogneiss is distinctively augen-rich; the K-feldspar augen range from 1-2 cm in diameter to >10 cm in diameter. The rock is pervasively deformed and on fresh surfaces the asymmetry of the fabric elements can be investigated to determine the shear sense recorded. It can be difficult, however, to determine the orientation of the stretching lineation and the appropriate observation surface for shear indicators.

Though not immediately apparent in outcrop the orthogneiss is intruded by leucocratic dykes. These dykes can be observed in the cliff face above the outcrop (Figure 14A).

If you continue on from this outcrop to the east and make your way up to the top of the talus cone, there is an excellent washed exposure of the augen orthogneiss near a small waterfall (Figure 14B). The outcrop here provides a three dimensional view of the augen and the potential asymmetry they demonstrate. Notably absent in this washed exposure is evidence of any intrusive rocks similar to those noted in the cliff face.

#### Stop 20 – Intruded Metasedimentary Rocks (N27.87843°, E086.44570°)

This location is structurally above the main orthogneiss unit, in a migmatitic quartzo-feldspathic gneiss with foliation-parallel leucosome. The leucosome is locally prone to recessive weathering giving the outcrop a pitted or rough appearance. The country rocks are cross-cut by a series of leucogranite dykes (Figure 14C) of variable thick-

ness. The dykes themselves weather more readily than the rocks they intrude, making them fairly conspicuous. The same relationship between leucogranite dykes and rocks at a similar structural level is observed in the upper Tama Kosi valley (Larson, 2012). Preliminary monazite and xenotime ages from the main intrusive phase above the dykes at the structurally highest level in the region indicate that it is Early Miocene in age (J. Cottle pers. comm.). The dykes noted in the previous study (Larson, 2012) and those noted here have the same mineral content as the main plutonic body and as such are likely part of the same intrusive event. If so, that would imply that deformation and development of the foliation in this region occurred prior to the Early Miocene.

#### Stop 21 – Metasedimentary Rocks (N27.87796°, E086.45030°)

This stop is just a bit farther along the cliff-side to the east. Here a very similar metasedimentary assemblage is preserved, with well-defined layering (Figure 14D), perhaps reflecting transposed primary compositional variation. Thin granitic dykes are also observed at this location and cross-cut the dominant foliation at a high angle (Figure 14E).

#### Stop 22 – Cross-cut Augen Orthogneiss – (N27.87124°, E086.44103°)

For the final stop of this field trip we cross to the other side of the valley and part way up the trail leading to Yalung La. Here we have moved structurally below the metasedimentary rocks of the past few stops and back into the augen orthogneiss unit. A unique aspect of this outcrop, however, is that the orthogneiss is cut by coarse-grained feldspar + quartz + tourmaline ± muscovite leucogranite dykes (Figure 14F). These dykes are similar in character to those observed structurally higher and, if the interpretation of the age of those dykes is correct, then it implies that the ductile deformation within the orthogneiss must predate the Early Miocene as well. Further work to more tightly constrain the timing of deformation in this region is underway.

### Na

It is suggested that the night be spent in Na once again. After a day of hiking around at high altitude the body will be glad for a rest before beginning



**Figure 14**

A) Leucogranite dykes (light diagonal streaks) visible in a cliff face above Na. B) Orthogneiss with large K-feldspar augen. C) Leucogranite dyke (recessive) cutting across the dominant tectonic foliation (from Larson, 2012; book is 11 cm across). D) Well-foliated paragneiss at high structural levels above the village of Na. E) Leucogranite dykes cutting across paragneiss (hammer is 36 cm long). F) Coarse-grained leucogranite dyke crosscutting augen orthogneiss.

the return trip. There is much to explore around the upper portion of the Rolwaling valley and many beautiful views to be seen. The steep valley walls also perform an admirable job of auto-sampling otherwise unreachable outcrops, bringing boulders to more accessible elevations. Moreover, this is an opportunity to examine Tso Rolpa and the engineering efforts that have been made to monitor and manage the lake.

## RETURN TRIP AND OPTIONAL EXTENSIONS

There are a number of options available for the return portion of the field trip. The simplest is to return along the path of approach. The walk down is quicker than walking up. It is possible to travel from Na to Dogang, Dogang to Jagat, Jagat to Shigati (or just past), and then Shigati to Dolakha in

four days. There is an enjoyable detour that can be taken from Gongar onto the ridge on the west side of the valley (Figure 1) towards the town of Bulung. This is a trail little traveled by trekkers and merges back with the main trail/road at Suri Dobhan.

Alternatively, a return path can be charted that crosses over Tashi Lapsa (5755 m), the divide between the Rolwaling valley and the Khumbu region. This pass, however, is notably dangerous and may require ropes and crampons to navigate depending on the time of year. A different pass, Yalung La, which exits the south side of the valley just above Na may also be attempted. Again, success is largely dependent on the weather conditions at the time. We tried for two years to get over this pass and were beaten back both times by heavy snowfalls. The Yalung La exits into the upper Khare Khola, which meets up with the Tama Kosi at the town of Suri Doban (Figure 1).

The field trip may also be extended by heading into the upper Tama Kosi valley north of Lama-bagar. This area is restricted and requires special access permits.

## ACKNOWLEDGEMENTS

The logistical efforts of Teke and Pradap Tamang of Pike Peak Trekking and a host of capable, affable support staff made this project possible. Alicia, Josh, and Dale Larson supplied support, company and field modeling duties. This research was supported by faculty start-up grants awarded by the University of Saskatchewan and the University of British Columbia and a Natural Sciences and Engineering Research Council Discovery Grant awarded to K. Larson. This guide benefited from careful readings by R. Law and R. Carosi.

## REFERENCES

- Beaumont, C., Jamieson, R.A., Nguyen, M., and Lee, B., 2001, Himalayan tectonics explained by extrusion of a low-viscosity crustal channel coupled to focused surface denudation: *Nature*, v. 414, p. 738–742.
- Carosi, R., Montomoli, C., Rubatto, D., and Visona, D., 2010, Late Oligocene high-temperature shear zones in the core of the Higher Himalayan Crystallines (Lower Dolpo, western Nepal): *Tectonics*, v. 29, (doi:10.1029/2008TC002400)
- From, R.E. and Larson, K.P., In Press, Tectonostratigraphy, deformation, and metamorphism of the Himalayan mid-crust exposed in the Likhu Khola region, east-central Nepal: *Geosphere*.
- Godin, L., Grujic, D., Law, R.D., and Searle, M.P., 2006, Channel flow, ductile extrusion and exhumation in continental collision zones: An introduction, in Law, R.D., Searle, M.P. and Godin, L. (eds) *Channel flow, ductile extrusion and exhumation in continental collision zones*, Geological Society, London, Special Publication 268, p. 1–23.
- Goscombe, B., Gray, D., and Hand, M., 2006, Crustal architecture of the Himalayan metamorphic front in eastern Nepal: *Gondwana Research*, v. 10, p. 232–255, (doi:10.1016/j.gr.2006.05.003).
- Groppo, C., Rolfo, F., and Indares, A., 2012, Partial Melting in the Higher Himalayan Crystallines of eastern Nepal: the effect of decompression and implications for the Channel Flow model: *Journal of Petrology*, (doi:10.1093/petrology/egs009).
- Heim, A. and A. Gansser (1939), *Central Himalayas: Geological Observations of the Swiss Expedition, 1936*, 245 pp., Memoir Society Helvetica Science.
- Ishida, T., 1969, Petrography and structure of the area between the Dudh Kosi and the Tamba Kosi, east Nepal: *Journal of the Geological Society of Japan*, v. 75, p. 115–125.
- Ishida, T. and Ohta, Y., 1973, Ramechhap-Okhaldunga region, in Hashimoto, S. et al., (eds) *Geology of the Nepal Himalayas*, Saikon Publishing Company, p. 39–68.
- Jamieson, R.A., Beaumont, C., Medvedev, S., and Nguyen, M.H., 2004, Crustal channel flows: 2. Numerical models with implications for metamorphism in the Himalayan-Tibetan orogeny: *Journal of Geophysical Research*, v. 109, B06407, (doi:10.1029/2003JB002811).
- Kellett, D.A., and Godin, L., 2009, Pre-Miocene deformation of the Himalayan superstructure, Hidden valley, central Nepal: *Journal of the Geological Society, London*, v. 166, p. 261–275, (doi:10.1144/0016-76492008-097).
- Kellett, D.A., Grujic, D., Coutand, I., Cottle, J., and Mukul, M., 2013, The South Tibetan detachment system facilitates ultra rapid cooling of granulite-facies rocks in Sikkim Himalaya: *Tectonics*, v. 32, (doi:10.1002/tect.20014).
- Larson, K., 2012, The geology of the Tama Kosi and Rolwaling valley region, East-Central Ne-

- pal: *Geosphere*, v. 8, p. 507–517, (doi:10.1130/GES00711.1).
- Larson, K., and Godin, L., 2009, Kinematics of the Greater Himalayan sequence, Dhaulagiri Himal: implications for the structural framework of central Nepal: *Journal of the Geological Society, London*, v. 166, p. 25–43, (doi:10.1144/0016-76492007-180).
- Larson, K., Godin, L., and Price, R.A., 2010, Relationships between displacement and distortion in orogens: Linking the Himalayan foreland and hinterland in central Nepal: *Geological Society of America Bulletin*, v. 122, p. 1116–1134, (doi:10.1130/B30073.1).
- Larson, K., Gervais, F., and Kellett, D.A., 2013, A P–T–t–D discontinuity in east-central Nepal: Implications for the evolution of the Himalayan mid-crust: *Lithos*, v. 179, p. 275–292, (doi:10.1016/j.lithos.2013.08.012).
- Martin, A.J., DeCelles, P.G., and Gehrels, G.E., 2005, Isotopic and structural constraints on the location of the Main Central thrust in the Annapurna Range, central Nepal Himalaya: *Bulletin of the Geological Society of America*, v. 117, p. 926–944, (doi:10.1130/B25646.1).
- Means, W.D., 1989, Stretching faults: *Geology*, v. 17, p. 893–896.
- Montomoli, C., Iaccarino, S., Carosi, R., Langone, A., and Visona, D., 2013, Tectonometamorphic discontinuities within the Greater Himalayan Sequence in Western Nepal (Central Himalaya): Insights on the exhumation of crystalline rocks: *Tectonophysics*, v. 608, p. 1349–1370, (doi:10.1016/j.tecto.2013.06.006).
- Morgan, S., and Law, R.D., 2004, Unusual transition in quartzite dislocation creep regimes and crystal slip systems in the aureole of the Eureka Valley-Joshua Flat-Beer Creek pluton, California: a case for anhydrous conditions created by decarbonation reactions: *Tectonophysics*, v. 384, p. 209–231, (doi:10.1016/j.tecto.2004.03.016).
- Schelling, D., 1992, The tectonostratigraphy and structure of the eastern Nepal Himalaya: *Tectonics*, v. 11, p. 925–943.
- Searle, M.P., Law, R.D., Godin, L., Larson, K., Streule, M.J., Cottle, J.M., and Jessup, M.J., 2008, Defining the Himalayan Main Central Thrust in Nepal: *Journal of the Geological Society, London*, v. 165, p. 523–534, (doi:10.1144/0016-76492007-081).
- Searle, M.P., Cottle, J.M., Streule, M.J., and Waters, D.J., 2010, Crustal melt granites and migmatites along the Himalaya: melt source, segregation, transport and granite emplacement mechanisms: *Earth and Environmental Science Transactions of the Royal Society of Edinburgh*, v. 100, p. 219–233.
- Searle, M., 2013, Crustal melting, ductile flow and deformation in mountain belts: Cause and effect relationships: *Lithosphere*, (doi:10.1130/REL006.1).
- Streule, M.J., Searle, M.P., Waters, D.J., and Horstwood, M.S.A., 2010, Metamorphism, melting, and channel flow in the Greater Himalayan Sequence and Makalu leucogranite: Constraints from thermobarometry, metamorphic modeling, and U–Pb geochronology: *Tectonics*, v. 29, (doi:10.1029/2009TC002533).
- Tippet, C.R., 1984, Geology of a transect through the southern margin of the Foxe fold belt (mainly NTS 27B), central Baffin Island, District of Franklin. Geological Survey of Canada, Open File 1110.
- Yakymchuk, C., and Godin, L., 2012, Coupled role of deformation and metamorphism in the construction of inverted metamorphic sequences: an example from far-northwest Nepal: *Journal of Metamorphic Geology*, v. 30, p. 513–535.
- Yin, A., 2006, Cenozoic tectonic evolution of the Himalayan orogen as constrained by along-strike variation of structural geometry, exhumation history, and foreland sedimentation: *Earth Science Reviews*, v. 76, p. 1–131.
- Yin, A., and Harrison, T.M., 2000, Geologic evolution of the Himalayan-Tibetan orogen: *Annual Review of Earth and Planetary Sciences*, v. 28, p. 211–280.